Photo-Redox Mechanism for the Reaction of "Cation-like" Zirconocene Silyl Complexes with Silanes

Vladimir K. Dioumaev† and John F. Harrod*

Chemistry Department, McGill University, Montreal, Québec, Canada H3A 2K6

Received August 2, 1999

A kinetic study of the photochemical reaction of $[Cp_2Zr(\mu\text{-}SiH_2Ph)]_2^{2+}2[BBu_n(C_6F_5)_{4-n}]^-$ (**1**) with $PhCH_2SiH_3$ to give the analogous $PhCH_2SiH_2$ complex **2** was carried out using a combination of NMR and EPR spectroscopy to follow the rates of disappearance of reactants and the appearance of intermediates and products. The paramagnetic intermediate $[Cp_2Zr^{III}]^+[BBu_n(C_6F_5)_{4-n}]^-$ (**3**) is produced with a quantum efficiency of 0.96 ± 0.16 on irradiation of **1** with light having $\lambda < 450$ nm. The rate law and analysis of intermediates supports a Zr(IV)/Zr(III) redox mechanism in which the rate-determining step is photodecomposition of **1** to generate **3** and silyl radicals by homolytic dissociation. In the presence of excess $PhCH_2SiH_3$ **3** reacts rapidly to give products.

Introduction

The formation of Si−Si bonds by group 4 metallocene catalyzed dehydrocoupling of hydrosilanes has attracted considerable attention.[1,2] However, the molecular weights of polysilanes formed in dehydrocoupling reactions are still too low or marginal for most potential applications. A clearer understanding of the mechanisms of such reactions is thus a prerequisite to further progress.

The most widely accepted mechanism, formulated by Tilley and co-workers, consists of a two-step σ-bond metathesis process with fixed oxidation state for the metal (Scheme 1).[2−5] This mechanism is based on kinetic and structural studies of stable, monomeric silylzirconocenes and -hafnocenes.[3,4] Application of the σ-bond metathesis model provides some guidelines for an improvement in the reaction performance.[2b] The same mechanism has been extended to lanthanide and scandium catalysts on the basis of kinetic studies and of nonlocal density functional calculations.[6−8]

Investigations of titanocene catalysts reported by Harrod et al. suggest that the reaction mechanism may be more complicated. A number of mono- and dimetallic reduced titanocene(III) and mixed-oxidation-state titanocene(III)/(IV) and titanocene(II)/(III) compounds from reactions of titanocenes with silanes have been isolated and structurally characterized.[9] The relationship of these compounds to the active catalytic species has not been clearly established, but the fact that only reduced species are isolated or observed suggests that M(III) species may be intermediates in the catalytic cycle. In the cases of other group 4 metal catalyzed reactions of silanes, germanes, and stannanes, intense colors, indicative of the formation of lower oxidation state species, have also been observed, although no investigation of their role has been reported to date.[10]

In addition to the σ-bond metathesis mechanism, schemes involving metal−silylene and −silyl radical

Scheme 1. Tilley σ-Bond Metathesis Mechanism for Reactions of Silanes with Early-Transition-Metal Silylmetallocenes[2b] (R = Aryl, Alkyl; R′ = H, $(SiHR)_nH$)

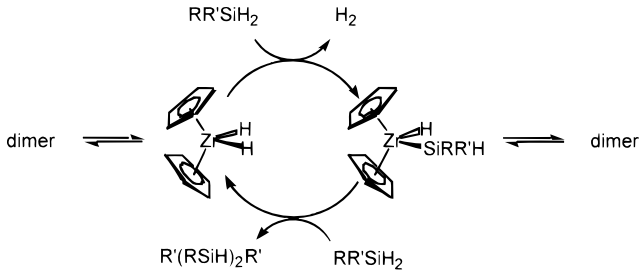

* To whom correspondence should be addressed. E-mail: harrod@omc.lan.mcgill.ca.

† Present address: Chemistry Department, University of Pennsylvania, Box 52, Philadelphia, PA 19104-6323. E-mail: dioumaev@sas.upenn.edu.

(1) (a) Harrod, J. F. In *Inorganic and Organometallic Polymers*; Zeldin, M., Wynne, K. J., Allcock, H. R., Eds.; American Chemical Society: Washington, DC, 1988; pp 89−100. (b) Harrod, J. F.; Mu, Y.; Samuel, E. *Polyhedron* **1991**, *10*, 1239. (c) Harrod, J. F. In *Inorganic and Organometallic Polymers with Special Properties*; Laine, R. M., Ed.; Kluwer Academic: Dordrecht, The Netherlands, 1992; Vol. 206, p 87.

(2) (a) Tilley, T. D. *Comments Inorg. Chem.* **1990**, *10*, 37. (b) Tilley, T. D. *Acc. Chem. Res.* **1993**, *26*, 22. (c) Tilley, T. D. In *Chemistry of Organic Silicon Compounds*; Patai, S., Rappoport, Z., Eds.; Wiley: New York, 1991; pp 245, and references therein.

(3) Woo, H.-G.; Tilley, T. D. *J. Am. Chem. Soc.* **1989**, *111*, 3757.

(4) Woo, H.-G.; Tilley, T. D. *J. Am. Chem. Soc.* **1989**, *111*, 8043.

(5) Tilley, T. D.; Woo, H.-G. *Polym. Prepr., Am. Chem. Soc. Div. Polym. Chem.* **1990**, *31*, 228.

(6) Forsyth, C. M.; Nolan, S. P.; Marks, T. J. *Organometallics* **1991**, *10*, 2543.

(7) Radu, N. S.; Tilley, T. D. *J. Am. Chem. Soc.* **1995**, *117*, 5863.

(8) Ziegler, T.; Folga, E. *J. Organomet. Chem.* **1994**, *478*, 57.

(9) (a) Samuel, E.; Harrod, J. F. *J. Am. Chem. Soc.* **1984**, *106*, 1859. (b) Aitken, C. T.; Harrod, J. F.; Samuel, E. *J. Am. Chem. Soc.* **1986**, *108*, 4059. (c) Samuel, E.; Mu, Y.; Harrod, J. F.; Dromzee, Y.; Jeannin, Y. *J. Am. Chem. Soc.* **1990**, *112*, 3435. (d) Gauvin, F.; Britten, J.; Samuel, E.; Harrod, J. F. *J. Am. Chem. Soc.* **1992**, *114*, 1489. (e) Harrod, J. F.; Mu, Y.; Samuel, E. *Can. J. Chem.* **1992**, *70*, 2980. (f) Britten, J.; Mu, Y.; Harrod, J. F.; Polowin, J.; Baird, M. C.; Samuel, E. *Organometallics* **1993**, *12*, 2672. (g) Woo, H. G.; Harrod, J. F.; Henique, J.; Samuel, E. *Organometallics* **1993**, *12*, 2883. (h) Xin, S.; Harrod, J. F.; Samuel, E. *J. Am. Chem. Soc.* **1994**, *116*, 11562.

(10) (a) Aitken, C.; Harrod, J. F.; Samuel, E. *Can. J. Chem.* **1986**, *64*, 1677. (b) Corey, J. Y.; Zhu, X.-H. *Organometallics* **1992**, *11*, 672. (c) Coutant, B.; Quignard, F.; Choplin, A. *J. Chem. Soc., Chem. Commun.* **1995**, 137. (d) Imori, T.; Lu, V.; Cai, H.; Tilley, T. D. *J. Am. Chem. Soc.* **1995**, *117*, 9931.

10.1021/om990609c CCC: $19.00
Publication on Web 01/28/2000

intermediates have also been proposed.[1a,11] However, the evidence in favor of these mechanisms is rather weak.

A photochemical exchange reaction of silanes with neutral silylzirconocenes and hafnocenes was reported by Tilley et al.[12] Paramagnetic products (presumably Zr^{III}) were detected, but the EPR peak intensities were low and the silane exchange reaction proceeded slowly even in the dark.[12] In a more recent study of the photochemically induced metathesis of CpCp*Hf(Cl)(Si(SiMe$_3$)$_3$ with $H_2Si(SiMe_3)_2$, it was concluded that reduction to Hf^{III} species was a key step, but neither their structure nor the reaction mechanism was investigated.[13]

The recurrent appearance of M^{III} species clearly undermines the hypothesis that dehydrocoupling occurs uniquely by a M^{IV} σ-bond metathesis mechanism and raises the possibility of mechanisms involving σ-bond metathesis at M^{III}, or redox cycles involving M^{III}/M^{IV}. We recently reported the catalytic dehydrocoupling of silanes with cation-like catalysts, Cp_2ZrCl_2/2BuLi/$(C_6F_5)_3B$ (Cp_2 = a variety of η^5-cyclopentadienyl ligands).[14,15] A stoichiometric reaction of Cp_2ZrCl_2/2BuLi/$(C_6F_5)_3B$ with $RSiH_3$ yields noncatalytic Zr^{IV} salts containing the dimeric cation $[Cp_2Zr(\mu\text{-}SiH_2R)]_2^{2+}$.[14−16] These dimers, while thermally quite stable, were shown to undergo a facile photolytic decomposition to produce Cp_2Zr^{III} complexes and a silyl radical.[16] The present paper describes a kinetic study of a model photochemical metathesis reaction between $[Cp_2Zr(\mu\text{-}SiH_2Ph)]_2^{2+}2[BBu_n(C_6F_5)_{4-n}]^-$ and $PhCH_2SiH_3$ which shows that an exchange of silyl substituents at the Zr center proceeds in a much more complex way than a single-step σ-bond metathesis process.

Results

Hydrosilane Exchange Reaction. Under ambient conditions in toluene, $[Cp_2Zr(\mu\text{-}SiH_2Ph)]_2^{2+}2[BBu_n(C_6F_5)_{4-n}]^-$ (**1**; Cp = η^5-cyclopentadienyl) and an excess of $PhCH_2SiH_3$ react almost quantitatively to give $[Cp_2Zr(\mu\text{-}SiH_2CH_2Ph)]_2^{2+}2[BBu_n(C_6F_5)_{4-n}]^-$ (**2**) and $PhSiH_3$ (eq 1). Traces (<1% based on initial [**1**]) of

$$\underset{\mathbf{1}}{[Cp_2Zr(SiH_2Ph)]_2^{2+}2[BBu_n(C_6F_5)_{4-n}]^-} \xrightarrow[-PhSiH_3]{h\nu,\ PhCH_2SiH_3} \underset{\mathbf{2}}{[Cp_2Zr(SiH_2CH_2Ph)]_2^{2+}2[BBu_n(C_6F_5)_{4-n}]^-} \quad (1)$$

$RSiH_2SiH_2R'$ (R, R′ = Ph, Bz) and H_2 are also produced. Likewise, $PhSiH_3$ reacts with **2** to produce **1**. The product **2** was identified by comparison to an independently synthesized sample.[17] The reaction only occurs in sunlight, or regular fluorescent light, and no reaction occurs in the dark over a period of 1 year. Once initiated, the reaction ceases if the light source is removed, showing it to be photochemical rather than photocatalytic.

The quantum yield for the overall reaction was measured to be 0.96 ± 0.16. Irradiation of the sample with monochromatic filtered light at different wavelengths showed that the observed photochemistry is due to light with a wavelength <440 nm. It gives rise to a number of EPR signals (vide infra) and a color change from colorless to yellow-brown. Both the color and the EPR signal intensities depend on the time of exposure and the intensity of the light source.

To clarify the role of light, three samples of **1** in toluene-d_8 were photolyzed simultaneously (see Experimental Section). Before the photolysis, only sample #1 contained $PhCH_2SiH_3$. In the case of sample #2, $PhCH_2SiH_3$ was added in the dark, after the completion of the photolysis. Sample #3 was a standard blank, subjected to the same photolysis conditions as the other two samples, but no $PhCH_2SiH_3$ was added at any point in the experiment. The total volume and the concentration of zirconium were maintained equal in all three samples both during and after the photolysis by adding appropriate amounts of $PhCH_2SiH_3$ or solvent.

On photolysis the concentration of **1** decreased in all three samples at the same rate and to the same extent. In sample #1 ($PhCH_2SiH_3$ present during photolysis) a complementary amount of **2** was formed, so that at the end of the photolysis cycle [**1**] + [**2**] = $[\mathbf{1}]_0$. When an excess of $PhCH_2SiH_3$ was added *in the dark* at the end of the photolysis cycle (sample #2), the rate of production of **2** was much slower than in the case of sample #1. The concentration of **2** in sample #2, however, slowly grew in the dark over a period of several weeks until it equaled that which would have been obtained if the irradiation had been carried out in the presence of $PhCH_2SiH_3$, as in sample #1.

In the absence of $PhCH_2SiH_3$ (sample #3), most of **1** is photolytically converted into NMR-silent, reduced zirconocene(III) products and $PhSiH_3$, which slowly revert back to **1** over a period of several months in the dark. Small amounts of an ^{1}H NMR-observable zirconocene species (singlet at 4.98 ppm; C_7D_8) are formed under these conditions, but this species has not been identified. The main NMR-silent compound is **3**, which has been observed, trapped, and identified earlier in the Cp_2ZrCl_2/BuLi/$(C_6F_5)_3B$ reaction.[16] Attempts to quantify the buildup of **3** by EPR spectroscopy were not successful for reasons which are described below.

In summary, the photolysis of **1** leads to the formation of **3**, which reacts rapidly with $PhCH_2SiH_3$ to produce the NMR-observable **2**. When $PhCH_2SiH_3$ is not immediately available to trap **3** as it forms, the latter reacts, with either itself or some other compound present in the mixture, to form a less reactive species. *The rate of decrease of concentration of **1** on irradiation is the same in both the presence and absence of $PhCH_2SiH_3$.*

Kinetic Study Using NMR Spectroscopy. A kinetic study was carried out on a model reaction of **1** with benzylsilane under pseudo-first-order rate conditions with respect to silane (eq 1). In the first series of experiments, the concentration of **1** was varied from

(11) (a) Aitken, C.; Harrod, J. F.; Gill, U. S. *Can. J. Chem.* **1987**, *65*, 1804. (b) Harrod, J. F.; Yun, S. S. *Organometallics* **1987**, *6*, 1381. (c) Harrod, J. F.; Ziegler, T.; Tschinke, V. *Organometallics* **1990**, *9*, 897.

(12) Woo, H.-G.; Heyn, R. H.; Tilley, T. D. *J. Am. Chem. Soc.* **1992**, *114*, 5698.

(13) Casty, G. L.; Lugmair, C. G.; Radu, N. S.; Tilley, T. D.; Walzer, J. F.; Zargarian, D. *Organometallics* **1997**, *16*, 8.

(14) Dioumaev, V. K.; Harrod, J. F. *Organometallics* **1994**, *13*, 1548.

(15) Dioumaev, V. K.; Harrod, J. F. *J. Organomet. Chem.* **1996**, *521*, 133.

(16) Dioumaev, V. K.; Harrod, J. F. *Organometallics* **1997**, *16*, 2798.

(17) Dioumaev, V. K.; Harrod, J. F. *Organometallics* **1996**, *15*, 3859.

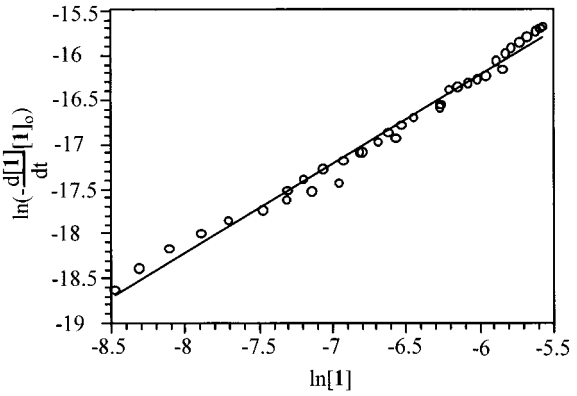

Figure 1. Kinetic plot for the reaction of **1** with $PhCH_2SiH_3$ as a function of rate vs concentration of **1**, showing the first-order dependence on [**1**]. Initial $[PhCH_2SiH_3]$ = 0.37 M. The line $y = -10.2(0.3) + [0.99(0.04)]x$ represents the least-squares fit to the data points (the quantities in parentheses are the 95% confidence limits; $R^2 = 0.987$).

0.000 95 to 0.0038 M and the initial concentration of benzylsilane was 0.37 M. Plots of $\ln(-[\mathbf{1}]_0\ d[\mathbf{1}]/dt)$ vs $\ln([\mathbf{1}])$, although somewhat scattered, show first-order dependence on **1** (Figure 1). The scattering of the data points can be attributed to the poor precision of fitting a polynomial to a small data set. The goodness of fit can be improved significantly by using a linear fitting procedure of imposing the first-order constraint and producing linear plots of $\ln([\mathbf{1}]/[\mathbf{1}]_0)$ vs time and k_{obsd} vs $1/[\mathbf{1}]_0$ (parts a and b of Figure 2). The choice of plots in which the rates or concentrations are normalized to $[\mathbf{1}]_0$ is dictated by the necessity to account for the fraction of visible light absorbed by reactants (see Experimental Section for details).

Another series of experiments was performed with a constant initial concentration of **1**, 0.0039 M, while the concentration of benzylsilane was varied from 0.10 to 1.20 M. The ln(−(initial rate)) vs $\ln([PhCH_2SiH_3])$ plot exhibits zero-order behavior in benzylsilane (Figure 3).

Finally, a series of identical samples ([**1**] = 0.0057 M; $[PhCH_2SiH_3]$ = 0.14 M) was subjected to different light intensities, by means of neutral density filters. The reaction rate shows a first-order dependence on the light intensity (Figure 4; the slope of the log−log plot is 0.89(0.05)). A combination of all of these experiments yields the rate law of eq 2.

$$d[\mathbf{1}]/dt = -k(10^{-a})[PhCH_2SiH_3]^0[\mathbf{1}]/[\mathbf{1}]_0 = -k_{obsd}[\mathbf{1}] \quad (2)$$

$[\mathbf{1}]_0$ = concentration at time = 0

a = optical density of a filter

Attempted Kinetic Study Using EPR Spectroscopy. A pure sample of **1** in toluene-d_8 was photolyzed, and the buildup of $[Cp_2Zr]^{\bullet+}$ concentration was monitored by EPR spectroscopy. The plot of the integral intensity of the EPR peaks vs photolysis time is roughly linear for about 30% of the reaction, and the rate of production of Zr^{III} species is close to the rate of a parallel reaction of **1** with $PhCH_2SiH_3$, using the same concentration of **1** and followed by NMR. This shows that the reduction step is not a minor side reaction but is an essential part of the reaction mechanism. It also shows that the rate-controlling step in the overall reaction (1) is most likely the step in which reduction to Zr^{III} occurs or a step which precedes reduction.

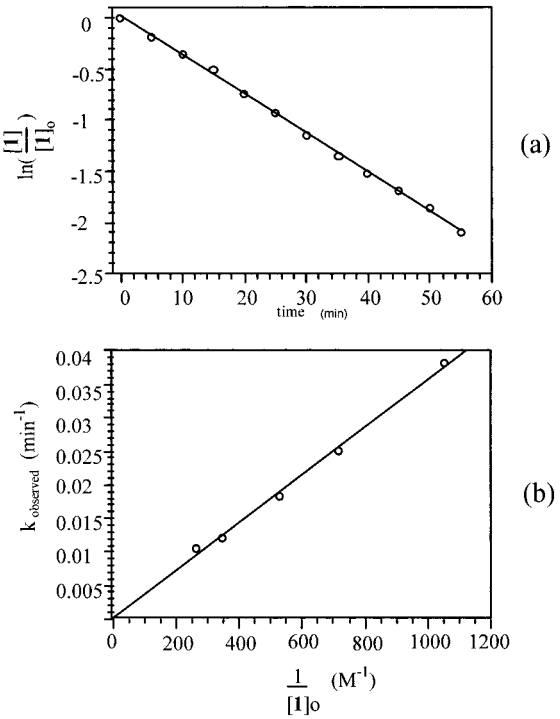

Figure 2. (a) Plot of $\ln\{[\mathbf{1}]/[I]_0\}$ as a function of time for the reaction of **1** with $PhCH_2SiH_3$, showing the first-order dependence on [**1**]. Initial [**1**] = 0.000 95 M; $[PhCH_2SiH_3]$ = 0.37 M. The line $y = 0.02(0.02) - [[3.81(0.07)] \times 10^{-2}]x$ represents the least-squares fit to the data points (the quantities in parentheses are the 95% confidence limits; $R^2 = 0.999$). (b) Plot of k_{obsd} vs $1/[\mathbf{1}]_0$, showing the inverse dependence on $[\mathbf{1}]_0$. Initial $[PhCH_2SiH_3]$ = 0.37 M. The line $y = 0.000(0.001) + [[3.5(0.2)] \times 10^{-5}]x$ represents the least-squares fit to the data points (the quantities in parentheses are the 95% confidence limits; $R^2 = 0.996$).

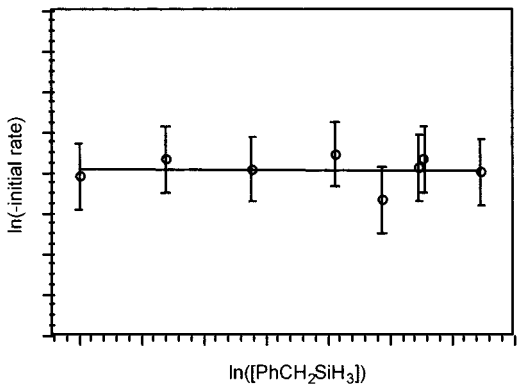

Figure 3. ln−ln plot of initial rate vs concentration of benzylsilane for the reaction of **1** with $PhCH_2SiH_3$, showing the zero-order dependence on $[PhCH_2SiH_3]$. Initial [**1**] = 0.0039 M. The bars indicate an ln(5%) = 1.6% error. The line $y = -9.99(0.07) - [0.00(0.04)]x$ represents the least-squares fit to the data points (the quantities in parentheses are the 95% confidence limits).

At longer photolysis times the increase in the concentration of EPR-observable Zr^{III} species in the reaction described in the preceding paragraph slows relative to the rate of decrease in **1**. This apparent lack of mass balance is attributed to the formation of an oligomeric, EPR-silent species, $\{Zr^{III}\}_n$, where n is an even number, most likely 2. Such a species, which has an even number

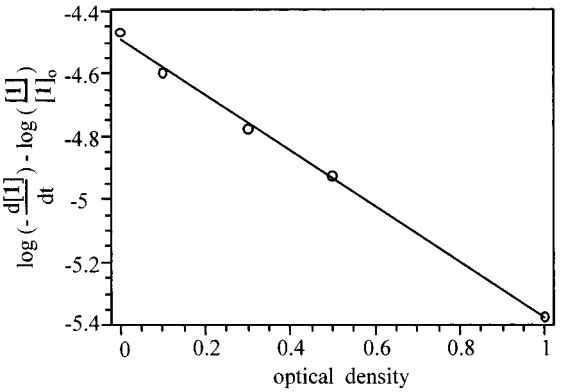

Figure 4. Kinetic plot for the reaction of **1** with $PhCH_2SiH_3$ as a function of rate vs optical density of the filters, showing the first-order dependence on light intensity. Initial [**1**] = 0.0057 M; $[PhCH_2SiH_3]$ = 0.14 M. The line $y = -4.49(0.02) - [0.89(0.05)]x$ represents the least-squares fit to the data points (the quantities in parentheses are the 95% confidence limits; $R^2 = 0.997$).

of electron spins, is expected to be antiferromagnetically coupled, but an equilibrium with the paramagnetic monomer, or some kind of dynamic rearrangement, could broaden any NMR resonances and render them poorly detectable. When a concentrated sample of **1** was photolyzed for a long time, extremely broad and featureless NMR resonances were observed.[16] The $\{Zr^{III}\}_n$ could result either from a thermal reaction or from a photochemically induced reaction of the strongly colored **3**. This problem does not arise in the NMR experiment, since the concentration of **3** remains low throughout the reaction in the presence of excess silane. The formation of a less reactive, polymeric $\{Zr^{III}\}_n$ species also explains why the reaction of $PhCH_2SiH_3$ with a preirradiated sample of **1** is much slower than the reaction of benzylsilane with **1** during irradiation. The secondary reaction of **3** frustrates a kinetic analysis based on EPR measurements. Thus, although the rate of a reaction of photochemically generated Zr^{III} with silane can be directly observed as a decay in the intensity of the EPR signal of **3**, it is not possible to evaluate it quantitatively since the $\{Zr^{III}\}_n$ species, whose concentrations and degrees of polymerization are unknown, also react with added silane.

A further complication is that the EPR-detectable monomer, i.e., **3**, is present as both tight-ion and solvent-separated-ion pairs.[16] Their signals appear as an overlapped and unresolved pair of EPR singlets, $g = 1.9964$, $a(Zr) = 7.1$ G and $g = 1.9972$, $a(Zr) = 12.3$ G, which interconvert with each other and gradually decay with different rates. In addition, there is another weak unresolved signal in the spectrum, $g = 2.0036$, possibly due to the silyl radicals,[16] whose decay also influences the intensity of the signals of **3**. An attempt was made to measure an overall decay rate, assuming that both forms of **3** obey the same rate law with similar rate constants. Contributions from the signal at $g = 2.0036$ were assumed to be negligible, as its intensity is weak. The plots of $\ln([Zr^{III}])$ vs time for the reaction of **3** with $PhCH_2SiH_3$ exhibited linear behavior, as expected for a first-order transformation of Zr^{III} to Zr^{IV}, and the goodness of fit within any given experiment was acceptable. However, ln(rate) vs $\ln([Zr^{III}])$ or ln(rate) vs $\ln([PhCH_2SiH_3])$ plots, obtained from a combination of different samples and experiments, showed poor reproducibility and precluded a rational kinetic analysis.

Scheme 2. Proposed Redox Mechanism for Reactions of Silanes with "Cation-like" Silylzirconocenes

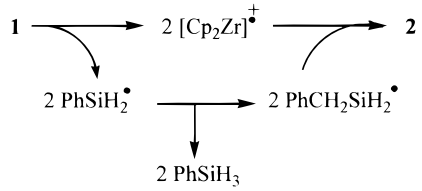

Despite the lack of a complete correspondence between the NMR and EPR results, it is clear that the initial rate of formation of **3** from **1** in the absence of silane (measured by EPR) matches the rate of the overall reaction of **1** into **2** in the presence of silane (measured by NMR). The EPR results at higher conversions, while conforming in a general way to those obtained by NMR measurements on reactions of **1** with $PhCH_2SiH_3$, do not consistently give the same kinetic parameters for different runs.

Discussion

Postulated mechanism. A minimal set of reactions, which fits the observed rate law and the observed products and intermediates under the various reaction conditions, is shown in Scheme 2. The transformation of **1** to **3** in Scheme 2 is almost certainly not a single-step process. However, the presently available information does not allow a detailed description of how it occurs. The zero-order dependence on $[PhCH_2SiH_3]$ and first-order dependence on [**1**] and on light intensity, I, together with the failure of **3** to accumulate in the system in the presence of excess silane all indicate that the rate-limiting step occurs within the left-hand reaction of Scheme 2. Analysis of this model yields the rate equation (2) (see Experimental Section for derivation).

A critical question with respect to eq 1 is the step, or steps, which involve light. Although dimeric zirconocene hydrides are known to undergo both dissociation to monomer and reduction upon photolysis, the actual photolytic step is unknown.[18] To the best of our knowledge there are no reported precedents for the photochemical cleavage of zirconocene dimers, but photochemical reductive elimination for monomeric early-transition-metal metallocenes is well-documented.[19] Photochemical reactions of monomeric, neutral silylzirconocene and silylhafnocene complexes with a hydrosilane have also been reported.[12,13] The observed quantum yield of unity in (1) constrains the mechanism to be one in which absorption of a single photon leads to the rupture of two Zr−Si bonds. At least two models (3) and (4), based in Scheme 2, fit the observed kinetic behavior. In (3), the primary photochemical step is a dissociation of the zirconocene dimer, in (4) it is homolysis of a Zr−Si bond.

(18) Knight, K. S.; Waymouth, R. M. *J. Am. Chem. Soc.* **1991**, *113*, 6268.

(19) (a) Uesaka, N.; Mori, M.; Okamura, K.; Date, T. *J. Org. Chem.* **1994**, *59*, 4542. (b) Knight, K. S.; Waymouth, R. M. *Organometallics* **1994**, *13*, 2575.; (c) Wischmeyer, U.; Knight, K. S.; Waymouth, R. M. *Tetrahedron Lett.* **1992**, *33*, 7735. (d) Knight, K. S.; Wang, D.; Waymouth, R. M.; Ziller, J. *J. Am. Chem. Soc.* **1994**, *116*, 1845. (e) Kablaoui, N. M.; Buchwald, S. L. *J. Am. Chem. Soc.* **1996**, *118*, 3182.

$$\{Zr^{IV}-Si\}_2 \xrightarrow[h\nu]{\text{slow}} 2\{Zr^{IV}-Si\} \xrightarrow{\text{fast}} 2\{Zr^{III}\} + 2Si^{\bullet} \quad (3)$$

$$\{Zr^{IV}-Si\}_2 \xrightarrow[h\nu]{\text{slow}} \{Zr^{IV}/Zr^{III}-Si\} + Si^{\bullet} \xrightarrow{\text{fast}} 2\{Zr^{III}\} + Si^{\bullet} \quad (4)$$

Mechanisms involving a *thermal* predissociation of **1** into monomeric zirconocene silyl are not likely in view of the absence of mixed dimers among the products of the photochemical reaction and the failure of an equimolar mixture of **1** and **2** to equilibrate in the dark. If the monomer−dimer equilibrium were a facile *thermal* reaction, one would expect the presence of both monomers (derived from **1** and **2**) in the reaction mixture and thence formation of the mixed zirconocene dimer $[Cp_2Zr(\mu\text{-}SiH_2Ph)(\mu\text{-}SiH_2CH_2Ph)ZrCp_2]^{2+}2[BBu_n(C_6F_5)_{4-n}]^-$. Although it may be argued that the heterodimer is thermodynamically much less stable than the homodimers, this seems to us to be unlikely.

In Scheme 2, the cascade of reactions which lead from **1** to **2** starts with a photoinduced decomposition of **1** and eventually produces two $PhSiH_2^{\bullet}$ radicals and two monomeric $[Cp_2Zr]^+$ ions (**3**). The $PhSiH_2^{\bullet}$ radicals then rapidly abstract H from the large excess of $PhCH_2SiH_3$ to give $PhCH_2SiH_2^{\bullet}$. Recombination of **3** with $PhCH_2SiH_2^{\bullet}$ followed by redimerization of the resulting $[Cp_2Zr^{IV}SiH_2CH_2Ph]^+$ completes the reaction.

An alternative mechanism for the conversion of **3** to **2** is the abstraction of H from $RSiH_3$, to give $[Cp_2Zr^{IV}H]^+$ (**4**) followed by a σ-bond metathesis between **4** and $PhCH_2SiH_3$ to generate **2** and H_2, as shown in (5) and (6). There is no question that the reaction can be forced

$$[CpZr]^{\bullet+} + PhCH_2SiH_3 \rightarrow [Cp_2ZrH]^+ + PhCH_2SiH_2^{\bullet} \quad (5)$$

$$[Cp_2ZrH]^+ + PhCH_2SiH_3 \rightarrow [Cp_2Zr(SiH_2CH_2Ph)]^+ + H_2 \quad (6)$$

to go via **4**. In the case of a preirradiated sample there are no silyl radicals present by the time $PhCH_2SiH_3$ is added. Nevertheless, the EPR signal of **3** disappears instantaneously when the sample is treated with $PhCH_2SiH_3$, presumably to produce **4**. Furthermore, an independently synthesized sample of **4** reacts rapidly with $PhCH_2SiH_3$ to produce **2.**[16]

If the conversion of **1** to **2** occurs by the reactions (5) and (6), the overall stoichiometry of the reaction changes from that shown in (1) to that shown in (7). The fact

$$\underset{\mathbf{1}}{[Cp_2Zr(SiH_2Ph)]_2^{2+}[BBu_n(C_6F_5)_{4-n}]_2^{2-}} + 3PhCH_2SiH_3 \xrightarrow{h\nu} \underset{\mathbf{2}}{[Cp_2Zr(SiH_2CH_2Ph)]_2^{2+}[BBu_n(C_6F_5)_{4-n}]_2^{2-}} + PhSiH_3 + H_2 + (PhCH_2SiH_2)_2 \quad (7)$$

that only traces of H_2 or disilanes were detected by NMR when **1** was photolyzed in an excess of $RSiH_3$, and only small amounts (1−5 mol %) when the photolysis was carried out in the absence of $PhCH_2SiH_3$, suggests that, at best, reactions 5 and 6 constitute a minor pathway in the overall reaction. Alternatively, there may either

Scheme 3 Redox Cycle for Dehydrocoupling via Silyl Radicals (R = Aryl, Alkyl; R′ = H, $(SiHR)_nH$)[16]

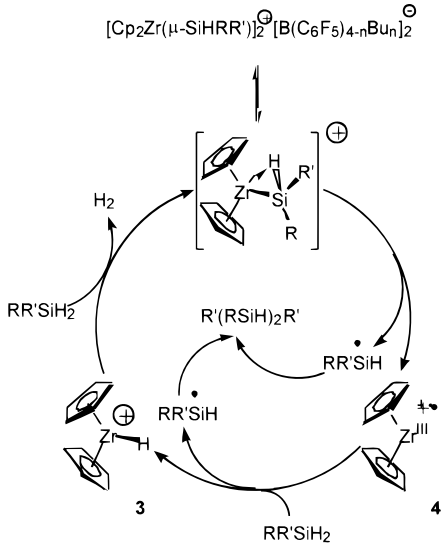

be a hitherto unidentified mechanism for the facile recycling of H_2 and a termination reaction of silyl radicals other than coupling, or the species $\{Zr^{III}\}_n$ may contain Si.

The alternative path of direct recombination of a $PhCH_2SiH_2^{\bullet}$ radical with **3**, as depicted in the right-hand side of Scheme 2, does not produce H_2. However, it does not fully conform to the experimental observations either. Thus, when **1** is photolyzed, there should be equal concentrations of **3** and $PhSiH_2^{\bullet}$ produced. In an excess of $PhCH_2SiH_3$ a fast hydrogen transfer would rapidly convert most of the $PhSiH_2^{\bullet}$ into $PhCH_2SiH_2^{\bullet}$. For a direct reaction of **3** and silyl radical, rate = $k_i[\mathbf{3}][RSiH_2^{\bullet}]$. $[PhSiH_2^{\bullet}]$ in the absence of $PhCH_2SiH_3$ and $[PhCH_2SiH_2^{\bullet}]$ in an excess of silane are similar. Hence, the rates of production of **1** in the former caseand **2** in the latter should also be similar. This is not, however, the case. When **1** is photolyzed in the absence of silane, it quickly disappears and is not regenerated at the rate **2** is produced in the presence of silane. Therefore, the recombination of **3** and $RSiH_2^{\bullet}$ must be slow in this concentration range.

Involvement of Silyl Radicals in Zirconocene-Catalyzed Dehydrocoupling Reactions. The proposed redox pathway, and the production of silyl radicals, leaves open the possibility that at least part of the Si−Si bond formation in group 4 metallocene catalyzed silane dehydrocoupling occurs by a chain to chain coupling of oligosilyl radicals, sustained by a cycle such as that shown in Scheme 3.[16] In the case of cation-like zirconocene-catalyzed polymerization of $PhSiH_3$ we believe that chain to chain coupling does occur to a significant extent. The GPC traces of polysilanes obtained with these catalysts are typically polymodal, with a number of poorly resolved peaks and shoulders, for which the molecular weights differ by a factor of ca. 2 between each neighboring peak. A typical example of such a GPC trace for a polyphenylsilane, produced with a $Cp_2ZrCl_2/2BuLi/B(C_6F_5)_3$ catalyst, is shown in Figure 5. This type of polymodality is expected for a condensation polymerization which has not proceeded far enough to give a smooth normal distribution of molecular weights. In the case of this catalyst the Zr is initially

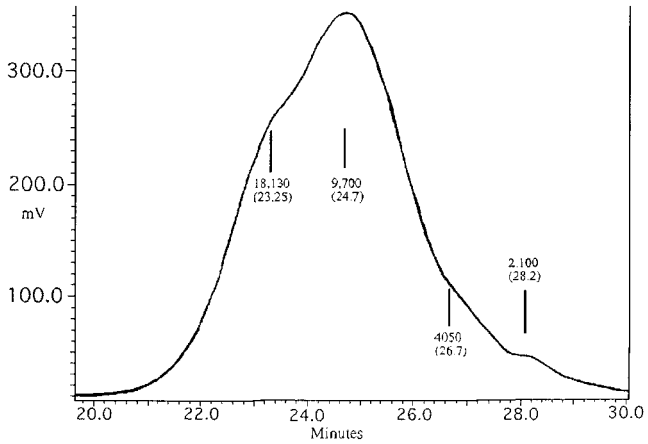

Figure 5. Typical GPC trace for a polyphenylsilane produced with a Cp_2ZrCl_2/2BuLi/$(C_6F_5)_3B$ catalyst. The markers show molecular weights (and retention times in parentheses).

mainly in the form of Zr^{III}, as a result of the thermal decomposition of $\{Zr^{IV}Bu\}$ species and not as a result of photolysis.[15,21]

Conclusions

Cationic silylzirconocene dimers, such as **1**, are rendered highly reactive toward silanes by irradiation with UV/vis light of $\lambda < 440$ nm. The quantum yield (0.96 ± 0.16 per zirconocene dimer), the experimentally obtained rate law (eq 2), and the fact that formation of **3** occurs at the same rate as the disappearance of **1** all support the conclusion that the first step of the sequence is a photochemical reaction of **1** which leads ultimately to the formation of two $PhSiH_2^{\bullet}$ radicals and two $[Cp_2Zr^{III}]^{+\bullet}$ ions. In the absence of excess silane, and in the presence of light, $[Cp_2Zr^{III}]^{+\bullet}$ reacts further to form an uncharacterized, probably polymeric, complex which only reacts very slowly in a thermal reaction with added silane.

In the presence of excess $PhCH_2SiH_3$, **3** formed by photolysis of **1** is captured in a rapid thermal reaction to give the product **2**. The manner in which this occurs remains obscure. From these results it is evident that, in any study of the zirconocene-catalyzed dehydrocoupling of silanes, possible involvement of light and of Zr^{III} must be considered. The polymodal molecular weight distributions already observed in certain cases (see Figure 5) support the hypothesis that chain growth by coupling of silyl radicals does occur.

Experimental Section

Materials and Methods. All operations were performed in Schlenk-type glassware on a dual-manifold Schlenk line, equipped with flexible stainless steel tubing, or in an argon-filled MBraun Labmaster 130 glovebox (<0.05 ppm of H_2O). Argon was purchased from Matheson (prepurified for the glovebox and UHP for the vacuum line) and used as received. Hydrocarbon solvents (protio- and deuteriotoluene) were distilled from Na/K alloy−benzophenone and stored in the glovebox. Silanes ($PhSiH_3$, $PhCH_2SiH_3$, and $PhSiD_3$) were synthesized according to the literature,[22] degassed, and stored over molecular sieves in the glovebox. Cp_2ZrCl_2, C_7D_8, C_6F_5-Br, PhC(O)Ph, BCl_3 (1.0 M in heptane), *n*-BuLi (1.6 M in hexanes), and $LiAlD_4$ were purchased from Aldrich and used as received, unless stated otherwise. Compound **1** was prepared by a previously published method.[14,15]

Physical and Analytical Measurements. NMR spectra were recorded on a Varian Unity 500 (FT, 500 MHz for ^1H) spectrometer. Chemical shifts for ^1H spectra were referenced using internal solvent references and are reported relative to tetramethylsilane. Quantitative NMR measurements were performed using residual solvent protons as internal references. Long repetition delay, 15 s (at least $5T_1$), was used to ensure complete magnetization relaxation and correct peak integration. EPR spectra were recorded on a Bruker ESP 300E (X-band) spectrometer and were referenced to external DPPH. Quantitative EPR measurements were performed with an external standard of TEMPO of known concentration. A number of experiments were done with different acquisition parameters (modulation and microwave power) to ensure that there was no saturation of the signal. The other acquisition parameters were compensated for by a system normalization constant and were usually kept constant for both the unknown and the standard sample measurements.

For the quantitative photochemical experiments, a general-purpose 9 W compact daylight fluorescent bulb (Sylvania, Model No. F9DTT/27K) with an output primarily in the 300−750 nm spectral region was used.[23] The lamp was placed in a homemade housing, equipped with a holder for an NMR tube (65 mm from the light source) and a window for a photofilter. The entire assembly was compact enough to fit in the thermostat of a gas chromatograph (HP 5890), which was used to control the reaction temperature to an accuracy of ±0.3 °C. For quantum yield measurements, the light intensity entering the photolysis cell (an NMR tube) through the band-pass filter (Corning CS-7-59) was determined by using the Reinecke's salt actinometer.[3] A typical photon flux into the photochemical cell was $(2.6 \pm 0.4) \times 10^{-5}$ einstein L^{-1} min^{-1}.

Photochemical Conversions of 1 to 2. All samples for NMR measurements were prepared in semidarkness, in the glovebox, and were loaded in Teflon-valved NMR tubes. A fractional dilution of stock solutions of **1** in C_6D_6 was used to ensure concentration accuracy. The following mixtures were prepared: (#1) [**1**] = 0.0057 M, 0.010 mL of $PhCH_2SiH_3$, total volume 0.490 mL; (#2 and #3) [**1**] = 0.0057 M, [$PhCH_2SiH_3$] = 0, total volume 0.490 mL. The samples were irradiated for 40 min in the glovebox. A 0.010 mL amount of $PhCH_2SiH_3$ was then added to sample #2 (approximately 0.14 M solution). Samples #1 and 3 were diluted with 0.010 mL of C_6D_6 to compensate for the concentration changes in sample #2. NMR measurements were performed 2 h after irradiation and repeated after 2 days and after 2 weeks.

The progress of the reaction of **1**-d_4 with $PhSiH_3$ and the appearance of disilanes were followed by monitoring the appropriate Si−H peaks of reactants and products by ^1H NMR. ^1H NMR for $PhSiH_nD_{3-n}$ (C_6D_6, +25 °C): δ 7.37 (m, *o*-Ph), 7.09 (m, *m*-Ph), 7.06 (m, *p*-Ph), 4.218 (s, $PhSiH_3$), 4.204 (s, $PhSiH_2D$) 4.198 (s, $PhSiHD_2$). ^1H NMR for $Ph(H)_2Si-Si(H)_2(CH_2Ph)$NMR ($C_6D_6$, +25 °C): δ 7.6−6.8 (m, Ph), 4.24 (m, $PhSiH_2$), 3.49 (m, $PhCH_2SiH_2$), 2.14 (t, 3.2 Hz, $PhCH_2$).

Kinetic Experiments Followed by NMR. All NMR samples were prepared in an NMR-tube assembly, consisting of an NMR tube fused to a Teflon valve. The samples were prepared in semidarkness, in the glovebox. A fractional dilution of stock solutions of **1** and benzylsilane in toluene-d_8 was used to ensure concentration accuracy. The samples were

(20) (a) Chatgilialoglu, C. *Chem. Rev.* **1995**, *95*, 1229. (b) Walsh, R. *Acc. Chem. Res.* **1981**, *14*, 246. (c) Dang, H.-S.; Roberts, B. R. *Tetrahedron Lett.* **1995**, *36*, 2875.

(21) Dioumaev, V. K.; Harrod, J. F. *Organometallics* **1997**, *16*, 1452.

(22) Finholt, A. E.; Bond, A. C.; Wilzbach, K. E.; Schlesinger, H. I. *J. Am. Chem. Soc.* **1947**, *69*, 2692.

(23) Rabek, J. F. *Experimental Methods in Photochemistry and Photophysics*; Wiley: Chichester, U.K., 1982; p 55.

loaded in the NMR-tube assembly, removed from the glovebox, and frozen, and the tubes were evacuated and flame-sealed in the dark. The following series were prepared: (#1) [$PhCH_2SiH_3$] = 0.37 M, [**1**] = 0.0038, 0.0029, 0.0019, 0.0014, and 0.00095 M; (#2) [**1**] = 0.0039 M, [$PhCH_2SiH_3$] = 1.20, 0.80, 0.60, 0.40, 0.20, and 0.10 M; (#3) five identical samples of [**1**] = 0.0057 M, [$PhCH_2SiH_3$] = 0.14 M.

The samples were kept in the thermostat for 10 min prior to irradiation (series #1 at 27.7 °C, #2 at 26.7 °C, and #3 at 30.0 °C) and then photolyzed for 5 min before transfer to the NMR probe, which was kept at the same temperature. No changes were detected in the sample when the irradiation was off. This irradiation-measurement cycle was repeated for every kinetic data point. The data were then plotted as concentration vs time, and a second-order polynomial fit procedure was applied to obtain the rate information.

Kinetic Experiments Followed by EPR. The photolytic EPR experiments were done either with the 9 W Sylvania lamp described above or with a Hg−Xe high-pressure arc, Hanovia 977B0010 520310, equipped with a water jacket to filter IR radiation, and a GM 252 Schoeffel Monochromator (Schoeffel Instruments Co., Westwood, NJ). The samples were prepared as described above, and the concentrations were verified by NMR measurements. The two lamps, and different irradiation periods, were used to generate different concentrations of Zr(III) species. The decay of the EPR signals was monitored, and the concentration was plotted vs irradiation time or vs time of decay. A second-order polynomial fit was applied to obtain the rate values. The following series was prepared: [**1**] = 0.0039 M; [$PhCH_2SiH_3$] = 0.80, 0.60, 0.50, 0.40, 0.20, 0.10, and 0.05 M.

Rate Law. If the first step is the rate-limiting photochemical reaction, the overall rate law is simply the rate of the photolysis of **1**:

$$\mathrm{d}[\mathbf{1}]/\mathrm{d}t = -\Phi(10^{-a})I_{\mathbf{1}}^{*} \tag{8}$$

where Φ is the quantum yield, a the optical density of a filter, and $I_{\mathbf{1}}^{*}$ the fraction of visible light ($\lambda < 440$ nm) absorbed by **1**

$$I_{\mathbf{1}}^{*} = I\epsilon_{\mathbf{1}}[\mathbf{1}]/\sum \epsilon_i[\mathbf{i}] \tag{9}$$

where ϵ_i is the extinction coefficient of the ith component and I is the fraction of visible light absorbed by the sample. Since the only compounds which have significant concentrations in the mixture and absorption bands in the specified spectral region are **1** and **2** ($[\mathbf{1}] + [\mathbf{2}] \cong [\mathbf{1}]_0$), and since they have similar extinction coefficients

$$I_{\mathbf{1}}^{*} \cong I[\mathbf{1}]/([\mathbf{1}] + [\mathbf{2}]) \cong I[\mathbf{1}]/[\mathbf{1}]_0 \tag{10}$$

Finally

$$\mathrm{d}[\mathbf{1}]/\mathrm{d}t = -\Phi(10^{-a})I[\mathbf{1}]/[\mathbf{1}]_0 \tag{11}$$

Acknowledgment. Financial support for this work from the NSERC of Canada and Fonds FCAR du Québec is gratefully acknowledged.

OM990609C